EnvironmentAsia
The international journal by the Thai Society of Higher Education Institutes on Environment

EnvironmentAsia 15(3) 2022 14-24
DOI 10.14456/ea.2022.44
ISSN 1906-1714; ONLINE ISSN: 2586-8861

Variation and Change of Hydro-Climatological Parameters in Iraq for the Period 1980-2019

Husam T. Majeed*, Dalia A. Mahmood, and Zahraa S. Mahdi

Department of Atmospheric Sciences, College of Science
Mustansiriyah University, Baghdad, Iraq

*Corresponding Author: hussam76@uomustansiriyah.edu.iq
Received: December 15, 2021; Revised: February 22, 2022; Accepted: May 30, 2022

Abstract

Extensive analysis of hydro-climatological parameters is essential for the management and strategies of water resources particularly in arid and semi-arid regions like Iraq. The aim of this work is to analyze and study the change and variations of the hydro-climatological parameters in Iraq during the past 40 years (1981-2020). Monthly means of hydro-meteorological variables were obtained from Fifth generation ECMWF atmospheric reanalysis of the global climate (ERA5). The data obtained included total precipitation (P), evaporation; including transpiration from vegetation (E), runoff; includes both surface and sub-surface (R), and potential evaporation (PE) for the period 1980-2019. Results showed considerable variations in the hydro-climatological parameters both in spatial and temporal scales. P and E were the maximum in the north and north eastern mountain areas and minimum in the western desert area. R only existed in the mountain areas. P in Iraq falls only during rainy season (October-May) and peaks during winter (December-February) while E and R occur during all month of the year and the peak amounts happen in May (for evaporation) and in April (for R) in the mountain area where melting snow is the major source of water. The spatiotemporal distribution of water storage indicated that all parts of Iraq in totally water deficit during the six months of April to September while the most significant water surplus occur in the three months of November-February. In Open water areas in Iraq, such as lakes and dam basins, E takes place all year around and therefore they are always in water deficit. Calculation of Aridity Index (AI) from annual PE and P indicated that Iraq can be divided into three climatic zones; a semi-arid zone (AI ranged from 0.2 to > 0.5) in the mountain areas, an arid zone (AI~ 0.2) in the foothills and eastern border areas, and a hyper arid zone (AI< 0.05) covering entire southern half of Iraq. Applying Mann-Kendall test on long term annual P, PE, and AI at four cities representing north, center, west, and south of Iraq showed that a negative trend in P and AI and positive trend in PE were observed but the trend of PE was the only one that was statistically significant.

Keywords: Precipitation; Evaporation; Potential evaporation; Water storage; Aridity Index; Iraq

1. Introduction

Water is essential for life on Earth. Although water resources appear abundant, only around 1% of it is readily available for human consumption. Due to the ever-increasing demands associated with exponential global population expansion, water resources are being prioritized globally. Water was prioritized to protect food, drinking water, fisheries, and the environment due to the world's growing population (Rahi and Halihan, 2010). Observational and historical hydrologic and meteorological data are used to plan water resource management initiatives (Chen *et al.,* 2007). In this regard, evaluating trends in hydrologic variables related to both hydrologic processes aids accurate water resource forecasting (Istanbulluoglu *et al.,* 2012), particularly in dry and semiarid regions

with high E and low rainfall volume (Rahi and Halihan, 2018; AL-Salihi, 2017). The law of mass conservation is used to the analysis of the water balance in hydrology. This asserts that the difference between total intake and output will be balanced by a change in water storage for any arbitrary volume and time period (Rahi and Halihan, 2018). The ability to estimate the effects of manmade changes in the regime of streams, lakes, and ground-water basins is aided by understanding the water balance (Mohajerani *et al.,* 2021). Precipitation (P) is considered on the input side of water balance calculations, while runoff; including both surface and sub-surface (R), evaporation; including transpiration from vegetation (E), and infiltration are considered on the output side. Its goal is arrived at the most accurate assessment of the situation. The water balance equation can be expressed as follows (Herrmann and Bucksch, 2014):

$$Input - Output = Change\ in\ Storage$$

In the water balance, P is the only input while output; include E, transpiration, and consumption. E is the loss of water from water surfaces or soil, whereas transpiration and consumption are examples of plant E. These two processes are known as potential evapotranspiration, which reflects water losses in areas when there is an abundance of water and may be computed using specialized equations. When the amount of water available is limited, E and transpiration are called actual evapotranspiration (Al-Sudani, 2018).

Water managers who are responsible for planning and adjudicating the allocation of water Resources must have a good understanding of the evapotranspiration process as well as knowledge of the spatial and temporal rates of evapotranspiration due to the variability of region and seasons Babir and Ali (2016) investigated the hydrological water budget of Koi Sanjaq Basin in northern Iraq. They distinguished three main unconfined aquifers in the study area and the flow direction was from northern and northeastern parts towards the south and southeastern parts (the Lesser Zab River). Their overall calculations of the water balance components showed that the groundwater recharge was 75.18 mm/year, representing 10.84 % of the total rainfall for the study area. AL-Kubaisi (2015) studied the water balance of the Mandali basin in east part of Iraq. Their results indicated that there were a three basic periods of climate variability wet period, semi wet and dry period. They found that the 60.8% water surplus in the basin which was equivalent to rainfall amount of 154.03 mm and the amount of R was 7.47 mm, and the amount of water recharge was 146.56 mm. Al-Kubaisi *et al.,* (2019) estimated the water balance for the central basin of Erbil Plain (North of Iraq). They used climatic data recorded in Erbil station for the period (1980-2016) to estimate evapotranspiration, water surplus, and water deficit. Their results indicated that there was water surplus of (79.18%) of the total rainfall (418 mm) based on the water balance and the water deficit represented (674.21mm) of the corrected potential evapotranspiration. Al-Sudani (2020) calculated the water balance in Iraq using meteorological data. His results showed that actual evapotranspiration depends directly on water while water surplus depends directly on both rainfall and actual evapotranspiration. Majeed and Al-Shammari (2019) assessed water balance of unconfined Aquifer in Karbala-Iraq. Their results exhibited that the flow direction is from the southwest to the northeast and east, towards the discharge zone along the Euphrates River. Their calculations of water balance showed that the inflow water that reach the study area was (6,317.57 m^3/day) while the amount of outflow water is (6931.93 m^3/day). Therefore, the change in the groundwater storage will be (-6,317.57 m^3/day). Al-Mohammdawi *et al.,* (2022) Assessed the spatial and temporal variations of terrestrial water storage of Iraq and calculate sustainability of water resources was generally low (range 0 – 0.36) and was higher in southern and western regions relative to northern and central areas of Iraq. Kheimi and Abdelaziz (2022) Calculated the daily evaporation in the model is also dependent on the distribution function, since the spatial variability of soil water storage affects the catchment-scale evaporation.

The aim of this work is to analyze and study the change and variations of the hydro-climatological parameters in Iraq

during the past 40 years (1980-2019). Analysis; include spatiotemporal long term variation, time series and statistical evaluation.

2. Materials and Methods

2.1 Study Area

Iraq is located between 29 °N and 38 °N in latitude and 38 °E and 49 °E in longitude, with a total area of around 437,072 km². Figure 1 depicts an elevation map of Iraq, which indicates that the country's topography may be separated into four distinct regions: the mountainous region in the north and northeast; the alluvial plains in the center and southeast; and the desert region in the southwest (Al-Ansari, 2021). Except in the north and northeast, where the Mediterranean climate prevails, Iraq's climate is mostly arid and semi-arid. In Iraq, the average annual P is around 215 mm. and only between October and May does P fall. Summer temperatures in the middle and southern portions of the country can exceed 50 °C, while winter temperatures in the north and mountain areas can drop below freezing (Shubbar *et al.,* 2017).

2.2 Data and Methodology

In this work monthly means of hydro-meteorological variables were obtained from ERA5 Global Reanalysis, European Center for Medium Range Weather Forecasts (ECMWF). ERA5 is the fifth generation ECMWF reanalysis for the global climate and weather (Bell et al., 2021). The data obtained included total P, E (including transpiration from vegetation), and R (includes both surface and sub-surface) for the period 1980-2019. The Grid Analysis and Display System (GrADS) were used to conduct the analysis. GrADS is an interactive desktop program for accessing, manipulating, and visualizing earth science data. GrADS is a free software provided by the Center for Ocean-Land-Atmosphere Studies, University of George Mason (http://cola.gmu.edu/grads/).

The law of water balance (Equation 1) asserts that inflows to any water system or area are equal to outflows plus storage change over time. Hence,

$$P = R + ET + \Delta S$$

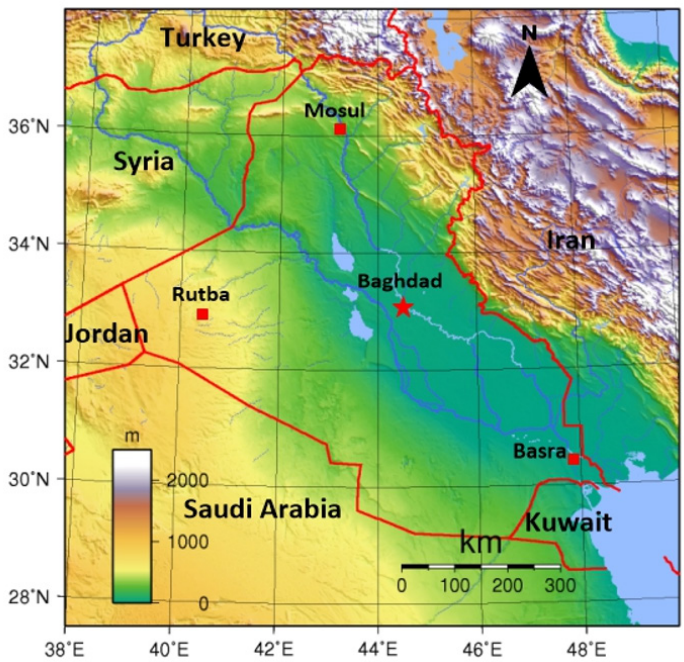

Figure 1. Study area. (http://www.diva-gis.org)

where P is the precipitation, R is the R (surface and sub-surface), ET is the evapotranspiration, and ΔS is the change in storage (in soil or the bedrock / groundwater). This equation has been used in this work to estimate ΔS from P, R, and ET monthly data for the period 1980-2019. Also time series have been generated for four cities representing different parts of the country. As seen in Figure 1, Mosul represents the north part, Baghdad, the capital and largest city is located at the center, the western desert plateau is represented by the town of Rutba and Basra, the second largest city, represents the south of Iraq. The geographic parameters of these four cities are given in Table 1.

The Aridity Index (AI) is a basic but useful numerical indicator of aridity that is derived as the ratio of annual P to annual potential E and is based on long-term climatic water shortages. The AI is a widely used metric for determining how dry a location's climate is. Arid areas or drylands are categorized into six subtypes using AI: cold, hyper-arid, arid, semi-arid, dry sub-humid, and humid are given in Table 2 (Stefanidis *et al.,* 2016).

Box and Whisker (McGill *et al.,* 1978) plot and Mann-Kendall (Gilbert, 1987) procedures were used to statistically evaluate the results and determine the significance of trends.

3. Results and Discussion

Results of the spatiotemporal distribution of the hydro-meteorological parameters over Iraq for the period 1980-2019 are shown in Figures 2 to 5. It is seen that the lowest P falls (few millimeters) on the western and south western desert area of the country and then gradually increases towards the mountain area in the north eastern part and towards eastern borders with Iran. The results also show that the Zagros Mountains, a long mountain range extends from southeastern Turkey and north eastern Iraq to western Iran, receives the highest P and the maximum P (> 160 mm/month) occur in Iraq during the months of Jan, Feb, and March. It is seen that P season in Iraq starts in October and ends in May. The spatiotemporal distribution of E (Figure 3) in Iraq indicates that high E result from lakes with a peak of around 180 mm during summer months. In general, the spatial distribution of E is comparable to that of P, i.e. areas of high P have high E while temporal distribution of E lags that of P, i.e. peak P occur in Jan-Mar while peak E occur in Apr. This is because soil becomes saturated after a long period of P during the cooler months and warmer temperature of Apr speeds up E. The white and light blue shadings in the Jan-Mar (in the Turkey-Iraq-Iran borders) which means no or very little E is an indicator of the presence of snow.

Table 1. The geographical parameters for selected stations

Station	Longitude (°E)	Latitude (°N)	Elevation (m)
Mosul	43.15	36.32	223
Baghdad	33.23	44.23	34
Rutba	33.03	40.28	615
Basra	30.57	47.78	2

Table 2. Aridity index for different climate types

Climate Type	Aridity Index
Dryland Subtypes	
Hyper-arid	AI < 0.05
Arid	0.05 < AI < 0.2
Semi-arid	0.2 ≤ AI < 0.5
Dry-Sub-humid	0.5 ≤ AI < 0.65
Non-Dryland	
Humid	AI ≥ 0.65
Cold	PE < 400 mm

The results also display that E from lakes and rivers occur during all months of the year. Figure 4 illustrates the spatiotemporal distribution of the total R (both surface and subsurface) in Iraq. It is obvious that the R in Iraq exists along the mountain area and the peak occur during spring months (Mar-May) the major contribution to the R come from melting snow. The water storage was calculated using the water balance equation and the results are displayed in Figure 5. It is clear that all lakes are characterized by water deficit during all months of the year and its maximum value in summer and minimum in winter. During the period from April to September there were water of 0 - 20 mm/month in the alluvial plain desert areas while in foothills and mountain areas the water deficit has relatively high values with maximum of 160 mm during April and May near the borders with Turkey and Iran. From October to January there were water surplus all over the country. In Feb only the mountain area has a water surplus and during March the water storage was between 0 - 20 mm in the north and south and -20 - 0 in the center.

Potential E is the amount of E that would occur if a sufficient water source were available. This parameter is affected by surface type, air temperatures, solar radiation, and wind. Figure 6 gives the spatiotemporal distribution of potential E in Iraq. It is clear that this parameter is low during winter and high during summer and reaches its minimum in the mountain area and its maximum values in the alluvial plain between Tigris and Euphrates rivers. To determine the aridity in Iraq the aridity index was calculated from annual P and annual potential E. The results are shown in Figure 7. The annual P average gradually extends from under 100 mm in the south western desert to more than 1250 mm on the top of the mountains in the north eastern region. The distribution of the annual average

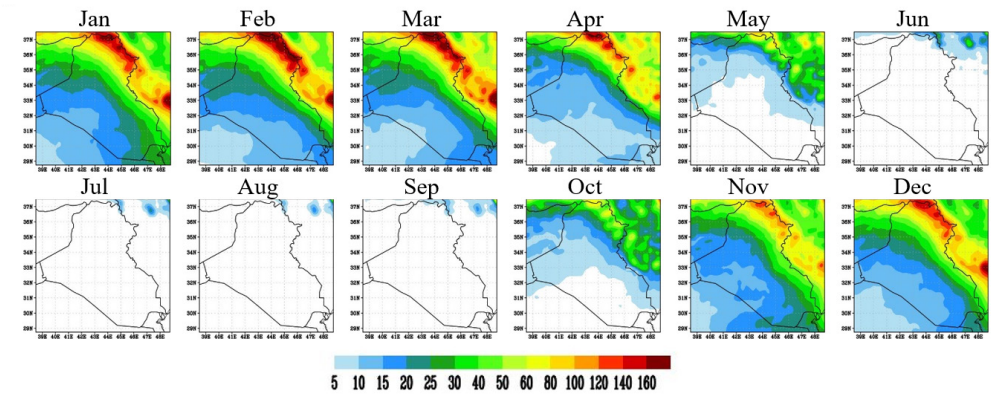

Figure 2. Long term spatiotemporal distribution of precipitation in Iraq for 1980-2019

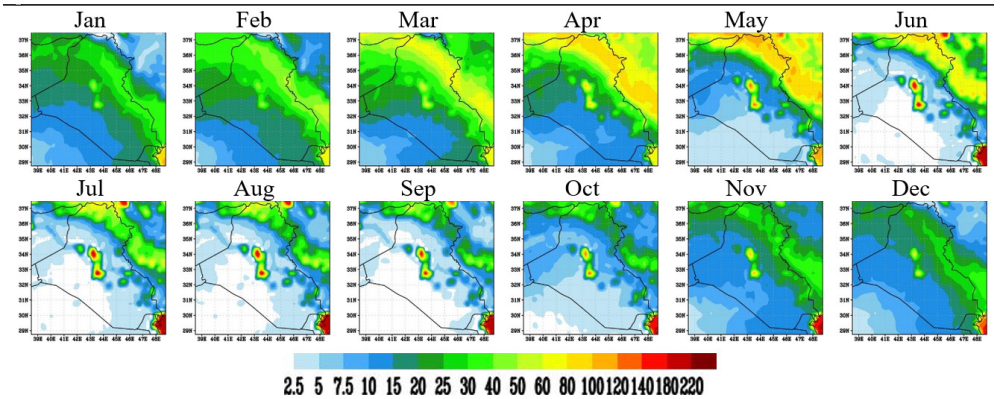

Figure 3. Long term spatiotemporal distribution of evaporation in Iraq for 1980-2019

of PE shows three distinctive areas of PE; low (< 2500 mm) in the north and western parts of Iraq, medium (< 3000 mm) in the central and southern parts around the alluvial plain and high (< 4000 mm) in the alluvial plain. It is notable that within this last area there a few patches of very high PE (3000 - 8000 mm) specially, around Baghdad and north of Basra. The distribution of the calculated AI shows that AI is < 0.05 over almost the entire southern half of Iraq indicating a hyper arid is prevailing in this area. AI increases gradually towards east (to the borders with Iran) and northeast towards the foothills and mountains and reach 0.2 at the edges of the mountains suggesting that an arid climate area. In the mountain area AI is from 0.2 to > 0.5 which is an indication of semi-arid climate. Also, in the mountain areas AI may reach more than 0.75 just over the border lines.

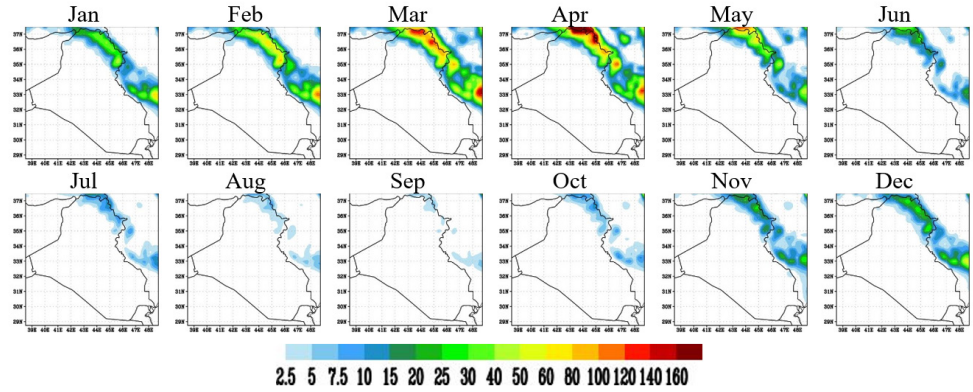

Figure 4. Long term spatiotemporal distribution of runoff in Iraq for 1980-2019

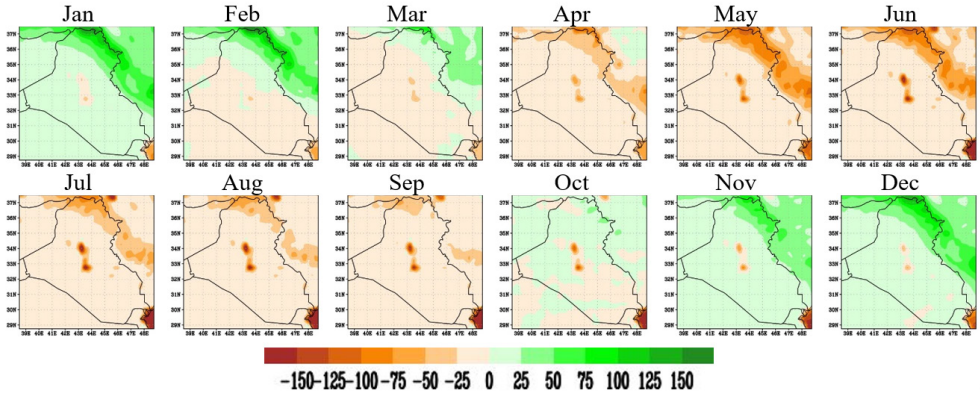

Figure 5. Long term spatiotemporal distribution of water storage in Iraq for 1980-2019

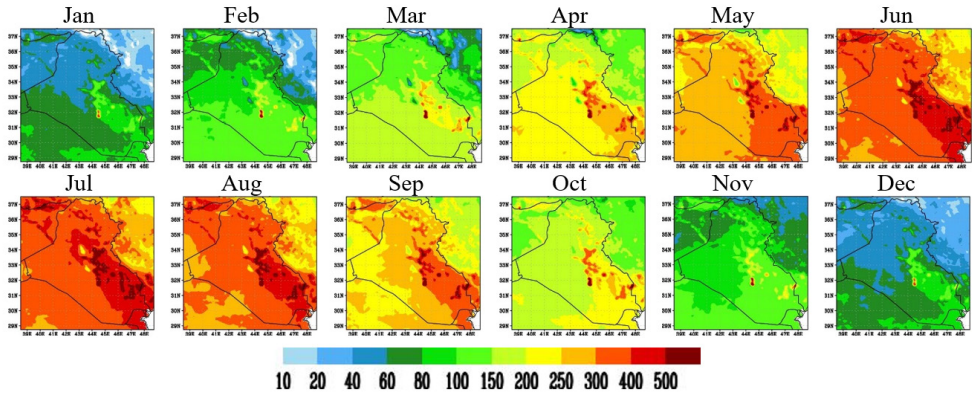

Figure 6. Long term spatiotemporal distribution of potential evaporation in Iraq for 1980-2019

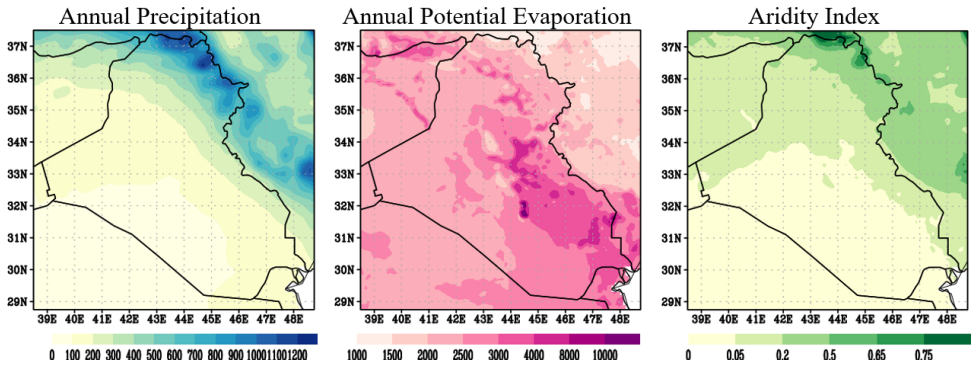

Figure 7. Averages of annual precipitation, annual potential evaporation, and aridity index in Iraq for 1980-2019

To investigate the trends of P, E, and water storage during the 40 years' period (1980-2019) monthly time series were constructed for the three variables at the four selected cities; Mosul, Baghdad, Rutba, and Basra. The results are displayed in Figure 8 and shows that P is quite variable and it varies from one year to another and no distinct trend is observed. Mosul receives the highest P followed by Baghdad, Basra, and Rutba. The E maps indicate that there is a time lag between high E and high P and this lag depends on many factors including the amount and period of P and surface temperature. Heavy P in short time period on a cool place led to relatively longer lags, such the case of Mosul while little P in longer period of time results in a very small time lag, such as the case of Rutba. The results also indicate that high E occurred during winter and spring in all four locations. During the last decade all parts of Iraq, excluding western high plateau where Rutba is located, were hit by many extreme to torrential rain events leading to unusual flooding in many parts of the country especially around Baghdad and southern part and thus increasing the water storage. The effects of these extreme events are apparent on the water storage maps of Baghdad and Basra during falls and winters of 2010-2019. Figure 9 presents the box and whisker plot of P, E, and water storage during 1980-2019 for the four cities. For P, the maximum observed was ~200 mm, ~75 mm, ~40 mm, and ~60 mm in Mosul, Baghdad, Rutba, and Basra respectively. In all four cities more than 50% of the data were below their mean value and most outliers (extreme) occur in Basra. For E, the (minimum, maximum) were (10, 105 mm), (2, 55 mm), (0, 36 mm), (2, 40 mm) for the four cities. Also more than 50% of the data were below their mean value and most outliers (extreme) occur in Basra. For water storage, the only box-whiskery plot that is statistically significant is the one for Mosul. This plot indicates that the maximum water surplus was 150 mm and minimum water deficit was 85 mm and 50 % of observation was below -10 mm. Only surplus outliers occurred in this city. For the other three cities the surplus and deficit are constrained within few millimeters around the median line at 0 mm but significant number of outliers was observed and the surplus outliers exceeded those of the deficit. Figure 10 illustrates the monthly time series for potential E. As the case in the spatiotemporal distribution the highest PEV occur in the southern city of Basra while less PEV happen in the western city of Rutba. It is notable that the significant variations in PEV over time occurred only during summer months (Jun-Aug) because of high solar radiation and a consequent high air and skin temperatures. Also, Shamal winds, a strong northwesterly winds, usually blow during summer in Iraq and greatly increasing the PEV Figure 11 gives the time series of annual P, annual potential E and annual AI for the four cities. The results show that AI oscillates between 0.2 and 0.45 in Mosul which indicates that the north of Iraq has semi-arid climate. In the other three cities the

majority of AI values are within 0.04 and 0.12 suggesting that an arid climate prevails over western, central, and southern parts of Iraq. Mann-Kendall test was performed on these annual time series to determine the significant of trends. The results listed in Table 3.

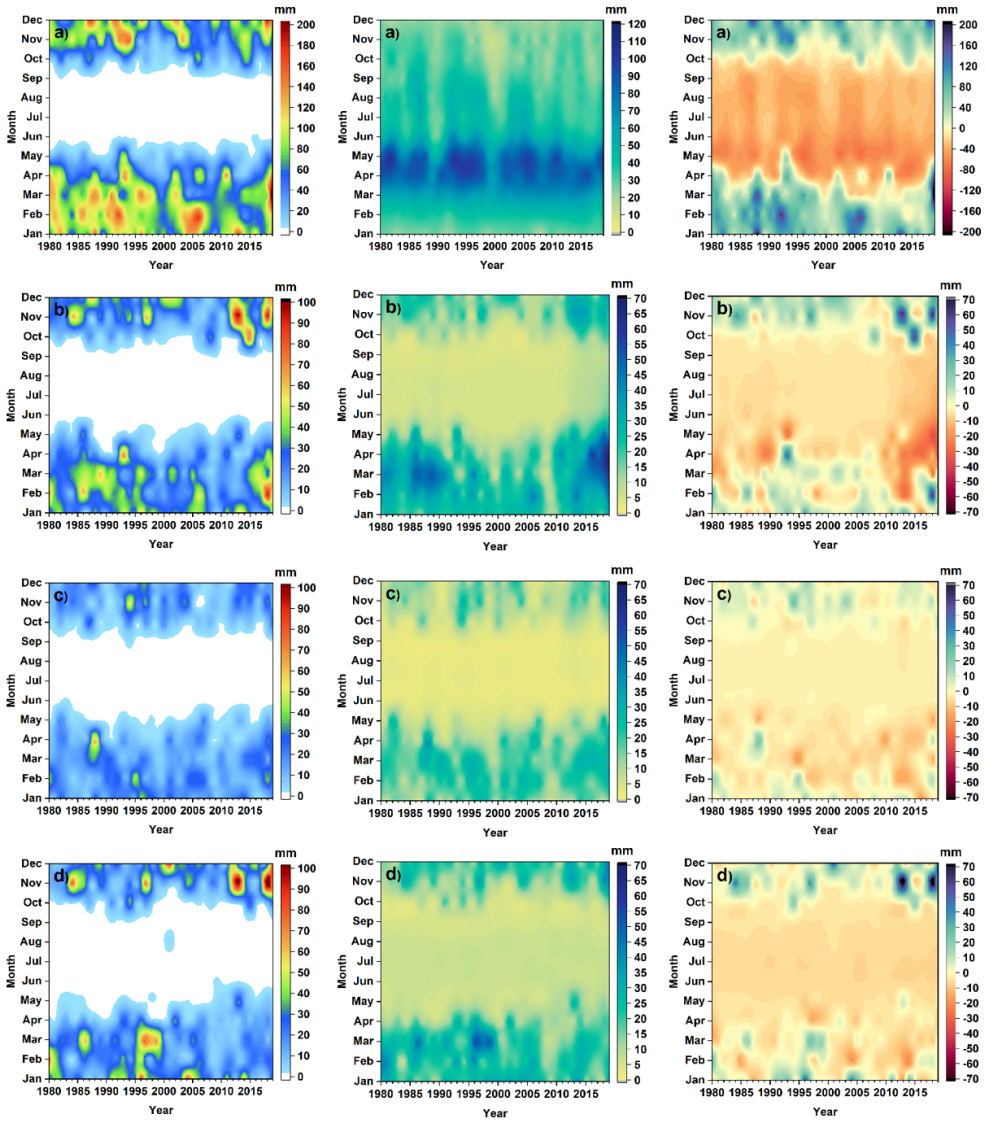

Figure 8. Long term monthly distribution of P (left panel), evaporation (middle panel), and water storage (right panel) for a) Mosul, b) Baghdad, c) Rutba, and d) Basra during 1980-2019

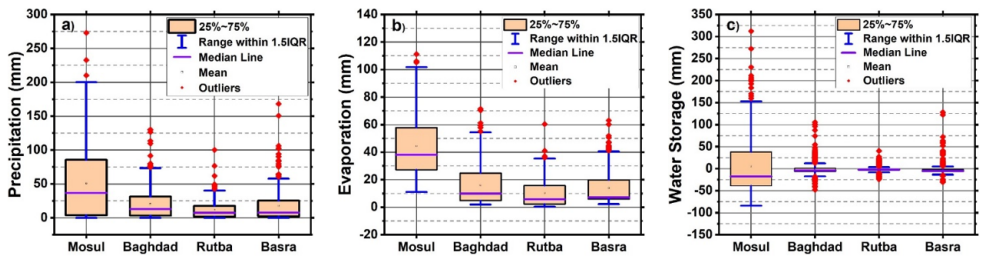

Figure 9. Box-Whisker plot of a) precipitation, b) evaporation and c) water storage for the four cities during 1980-2019

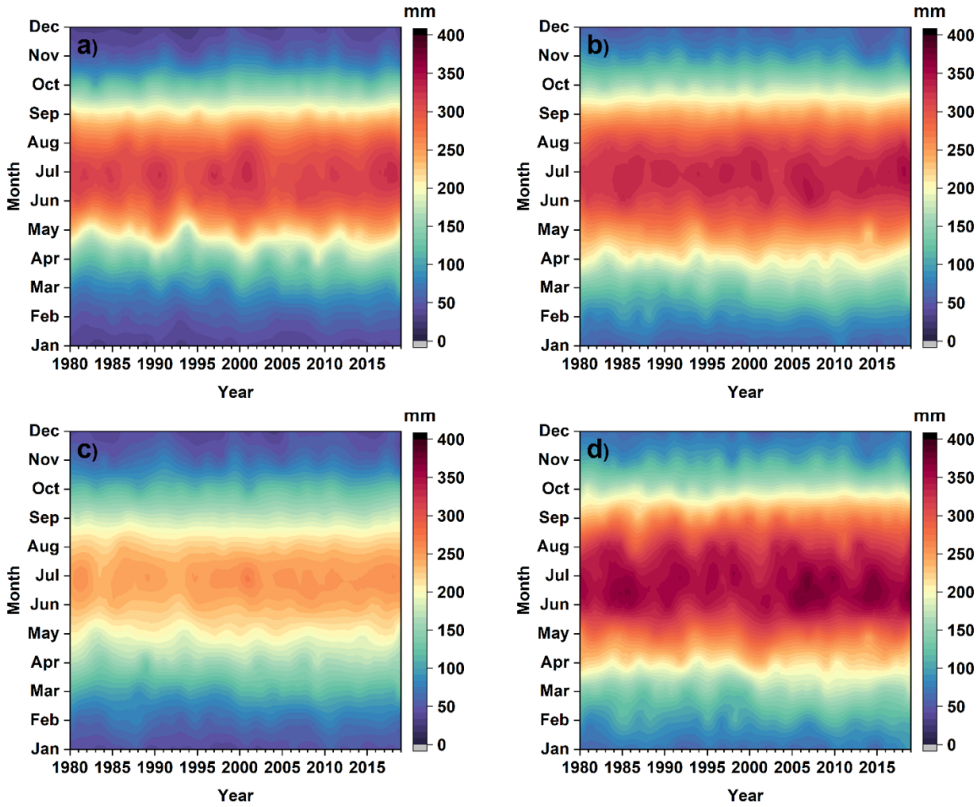

Figure 10. Long term monthly distribution of potential evaporation for a) Mosul, b) Baghdad, c) Rutba, and d) Basra during 1980-2019

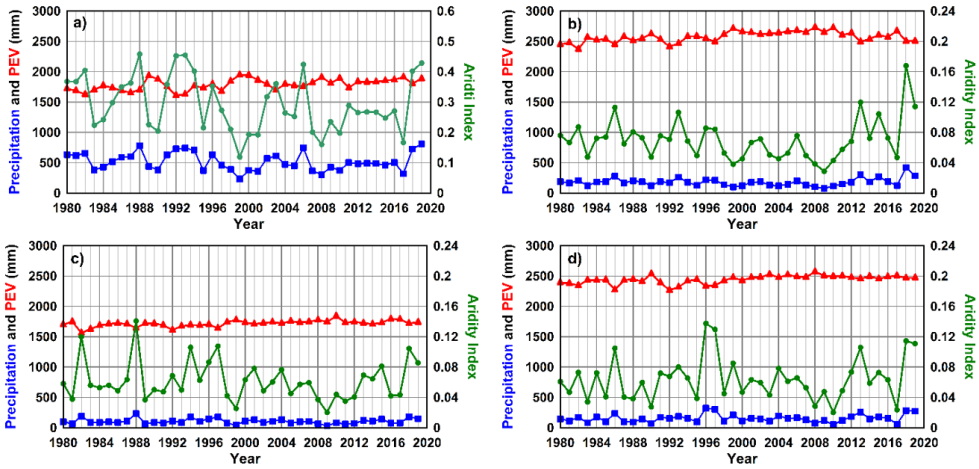

Figure 11. Annual average precipitation, potential evaporation, and aridity index for a) Mosul, b) Baghdad, c) Rutba, and d) Basra during 1980-2019

Table 3. Mann-Kendall test results

City	Time series	First year	Last year	n	Test Z	Significant.
Mosul	P	1980	2019	40	-0.97	
	PE	1980	2019	40	3.65	***
	AI	1980	2019	40	-1.46	
Baghdad	P	1980	2019	40	-0.13	
	PE	1980	2019	40	2.99	**
	AI	1980	2019	40	-0.57	
Rutba	P	1980	2019	40	-0.27	
	PE	1980	2019	40	3.76	***
	AI	1980	2019	40	-0.43	
Basra	P	1980	2019	40	1.04	
	PE	1980	2019	40	3.95	***
	AI	1980	2019	40	0.69	

P: Annual precipitation, PE: Annual potential evaporation, AI: Aridity index
** trend is significant at p = 0.01
*** trend is significant at p = 0.001

4. Conclusion

Iraq is experiencing a severe water scarcity, necessitating the exploration of all available water resources to supplement the country's water supply. As a result, finding solutions to water shortages becomes a top priority. In this work hydro- meteorological parameters over Iraq for the period 1980-2019 were analyzed to investigate the spatiotemporal distribution of water storage over different parts of the country. The results indicated that P is the major source of water storage while R (both surface and under surface) is significant only in the mountain areas and its peak occur during the spring months of March to May as a result of melting snow. Open water areas such as lakes and dam basins were characterized by water deficit during all months of the year due to high E rates especially during hot summer months (Jun-Aug). Results also reflected that water surplus occur during six months (Oct to Mar) while other warmer and dryer months are characterizing by water deficit. Both extremes of water surplus/deficit usually happen in the mountain areas. Calculations of Aridity Index (AI) showed that AI was < 0.05 over almost the entire southern half of Iraq indicating an area of hyper arid climate. At foothills and eastern border areas AI reached 0.2 suggesting that these areas have an arid climate. In the mountain area AI ranged from 0.2 to > 0.5 which is an indication of semi-arid climate.

Analysis of hydro-meteorological parameters at four cities representing north, center, west, and south of Iraq revealed that P is quite variable and it varies from one year to another and in general, the spatial distribution of E is comparable to that of P, i.e. areas of high P have high E while temporal distribution of E lags that of P, i.e. peak P occurs in Jan-Mar while peak E occurs in Apr. This is because soil becomes saturated after a long period of P during the cooler months and warmer temperature of Apr speeds up E. Box-whiskery plots exhibited that the only statistically significant water storage was found in the northern city of Mosul while in the other three cities the surplus and deficit were constrained within few millimeters around the median line at 0 mm but significant number of outliers were observed and the surplus outliers exceeded those of the deficit. These surplus outliers may be attributed to the extreme rain events that frequently occur over Iraq. Time series of annual P, annual potential E and annual AI for the four cities showed that AI oscillates between 0.2 and 0.45 in Mosul and in the other three cities the majority of AI values were within 0.04 and 0.12. Mann-Kendall trend test resulted in positive trend in PE and negative trend in Ps AI and the PE trend was the only statistically significant one.

References

Al-Ansari N. Topography and climate of Iraq. Journal of Earth Sciences and Geotechnical Engineering 2021; 11: 1-13.

Al-Kubaisi QY. Water balance of the basin of Mandali/east part of Iraq. Iraqi Journal of Physics 2015; 13: 51-57.

Al-Kubaisi QY, Hussain TA, Ismail MM, Abd-Ulkareem FA. Estimation of water balance for the central basin of Erbil plain (north of Iraq). Engineering and Technology Journal 2019; 37: 22-28.

Al-Mohammdawi JA, Al-Abadi AM, Al-Ali AK, Shahid S, Fryar A, Wang X. Assessing the spatial and temporal variations of terrestrial water storage of Iraq using GRACE satellite data and reliability–resiliency–vulnerability indicators. Arabian Journal of Geosciences 2020; 15: 342.

Al-Salihi AM. Impact of precipitation on aerosols index over selected stations in Iraq using remote sensing technique. Modeling Earth Systems and Environment 2017; 3: 861-871.

Al-Sudani HIZ. Study of Morphometric Properties and Water Balance Using Thornthwaite Method in Khanaqin Basin, East of Iraq. Journal of University of Babylon for Engineering Sciences 2018; 26: 165-175.

Al-Sudani HIZ. Calculation of meteorological water balance in Iraq. Resources Environment and Information Engineering 2020; 2: 84-89.

Babir GB, Ali SM. Hydrogeologic and water balance of Koi Sanjaq basin, northern Iraq. Iraqi Journal of Science 2016; 57: 423-435.

Bell B, Hersbach H, Simmons A, Berrisford P, Dahlgren P, Horányi A, Muñoz-Sabater J, Nicolas J, Radu R, Schepers D. The ERA5 global reanalysis: Preliminary extension to 1950. Quarterly Journal of the Royal Meteorological Society 2021;147: 4186-4227.

Chen H, Guo S, Xu CY, Singh VP. Historical temporal trends of hydro-climatic variables and runoff response to climate variability and their relevance in water resource management in the Hanjiang basin. Journal of hydrology 2007; 344: 171-184.

Gilbert RO. Statistical methods for environmental pollution monitoring. John Wiley & Sons; 1987.

Herrmann H, Bucksch H. Wörterbuch GeoTechnik/Dictionary Geotechnical Engineering: Deutsch–Englisch/German–English. Springer-Verlag; 2014.

Istanbulluoglu E, Wang T, Wright OM, Lenters JD. Interpretation of hydrologic trends from a water balance perspective: The role of groundwater storage in the Budyko hypothesis. Water Resources Research 2012; 48(3).

Kheimi M, Abdel-Aziz SM. A Daily Water Balance Model Based on the Distribution Function Unifying Probability Distributed Model and the SCS Curve Number Method. Water 2022; 14: 143.

Majeed SA, Al-Shmmari MM. Water Balance Assessment of Unconfined Aquifer (Karbala-Iraq). 2019 4th Scientific International Conference Najaf (SICN). IEEE 2019: 166-171.

Mcgill R, Tukey JW, Larsen WA. Variations of box plots. The american statistician 1978; 32: 12-16.

Mohajerani H, Zema DA, Lucas-Borja ME, Casper M. Understanding the water balance and its estimation methods. Precipitation. Elsevier; 2021.

Rahi KA, Halihan T. Changes in the salinity of the Euphrates River system in Iraq. Regional Environmental Change 2010; 10: 27-35.

Rahi KA, Halihan T. Salinity evolution of the Tigris River. Regional Environmental Change 2018; 18: 2117-2127.

Shubbar RM, Salman HH, Lee DI. Characteristics of climate variation indices in Iraq using a statistical factor analysis. International Journal of Climatology 2017; 37: 918-927.

Stefanidis K, Kostara A, Papastergiadou E. Implications of human activities, land use changes and climate variability in Mediterranean lakes of Greece. Water 2016; 8: 483.